N6-Methylandenosine-Related lncRNAs Play an Important Role in the Prognosis and Immune Microenvironment of Pancreatic Ductal Adenocarcinoma

YuHai Hu
First Affiliated Hospital of Fujian Medical University
YiPing Chen (cypgg@fjmu.edu.cn)
First Affiliated Hospital of Fujian Medical University

Research Article

Keywords: Pancreatic ductal adenocarcinoma, N6-methylandenosine, long non-coding RNA, prognostic signature, Immune

Posted Date: May 5th, 2021

DOI: https://doi.org/10.21203/rs.3.rs-274618/v2

Abstract

Background

Pancreatic ductal adenocarcinoma (PDAC) is a highly aggressive, fatal tumor. N6-methylandenosine (m6A) methylation is the major epigenetic modification of RNA including lncRNAs. The roles of m6A-related lncRNAs in PDAC have not been fully clarified. The aim of this study is to assess gene signatures and prognostic value of m6A-related lncRNAs in PDAC.

Methods

The Cancer Genome Atlas (TCGA) dataset and the International Cancer Genome Consortium (ICGC) dataset were explored to identify m6A-related lncRNAs. Univariate, least absolute shrinkage and selection operator (LASSO) and multivariate Cox regression were performed to construct the m6A-related lncRNAs prognostic riskscore (m6A-LPR) model to predict the overall survival (OS) in the TCGA training cohort. Kaplan–Meier curve with log-rank test and receiver operating characteristic (ROC) curve were used to evaluate the prognostic value of the m6A-LPR. Furthermore, the robustness of the m6A-LPR was further validated in the ICGC cohort. Tumor immunity was evaluated using ESTIMATE and CIBERSORT algorithms.

Results

A total of 262 m6A-related lncRNAs were identified in two datasets. In the TCGA training cohort, 28 prognostic m6A-related lncRNAs were identified and the m6A-LPR including four m6A-related lncRNAs was constructed. The m6A-LPR was able to identify high-risk patients with significantly poorer OS and accurately predict OS in both the TCGA training cohort and the ICGC validation cohort. Analysis of tumor immunity revealed that high-risk group had remarkably lower stromal, immune, and ESTIMATE scores. Moreover, high-risk group was associated with significantly higher levels of plasma B cells and resting NK cells infiltration, and lower levels of infiltrating resting memory CD4 T cells, monocytes and resting mast cells.

Conclusions

Our study proposed a robust m6A-related prognostic signature of lncRNAs for predicting OS in PDAC, which provides some clues for further studies focusing on the mechanism process underlying m6A modification of lncRNAs.

Introduction

Pancreatic ductal adenocarcinoma (PDAC) is a major histological subtype of pancreatic cancer. The incidence of PDAC is rising and the five-year survival rate is less than 5% with no significant improvement in survival over the past 10 years[1,2]. Surgical resection offers the only potentially curative treatment, but 80% of patients with PDAC are not amenable to surgery at diagnosis[3]. The efficacy of systemic treatment is limited and the advent of targeted and immune therapies are promising strategies to address this challenge. Thus, it is urgent to investigate potential therapeutic targets for PDAC.

N6-methylandenosine (m6A) RNA methylation is the main epigenetic modification of messenger RNAs (mRNAs) and non-coding RNAs (ncRNAs)[4], it has been confirmed to play critical regulatory roles in the modification of tumor RNAs[5]. M6A modifications are invertible and dynamical processes that are regulated by three kinds of m6A regulator, including methyltransferases (“writers”), signal transducers (“readers”) and demethylases (“erasers”)[6]. Recent studies demonstrated that m6A modification involves the regulation of oncogenesis and tumor progression in PDAC[7–12]. ALKBH5 serves as a PDAC suppressor by regulating the posttranscriptional activation of PER1 through m6A abolishment[7] and decreasing WIF-1 RNA methylation and mediating Wnt signaling[9]. Upregulation of METTL14 can promote the growth and metastasis of PDAC by decreasing of PERP levels[11].

Long non-coding RNAs (lncRNAs) regulate the biological functions of cells, including the proliferation, infiltration and metastasis of certain tumor cells[13], and dysregulation of lncRNAs had been reported to play a crucial role in the carcinogenicity of PDAC[8,14–16]. A recent study found that m6A reader IGF2BP2 regulates lncRNA DANCR to promote cancer stemness-like properties and pancreatic cancer pathogenesis[8]. Nevertheless, the full impact of m6A regulators on the aberrant lncRNAs expression in cancers is still unclear and few studies have been conducted to investigate the mechanisms underlying how lncRNAs are regulated by m6A modification to involve in the onset and development of PDAC. Therefore, understanding how m6A modifications of lncRNAs contribute to PDAC progression can help to identify novel biomarkers as potential therapeutic targets.

In this study, The Cancer Genome Atlas (TCGA) dataset (n = 140) and the International Cancer Genome Consortium (ICGC) dataset (n = 63) were explored to identify 262 m6A-related lncRNAs in patients with PDAC. Then we found that 28 prognostic m6A-related lncRNAs in TCGA cohort and we constructed an m6A-related lncRNAs prognostic riskscore (m6A-LPR) model including four prognostic m6A-related lncRNAs to predict the overall survival (OS) of patients with PDAC. The relevance of the m6A-LPR with tumor immunity was also evaluated. Our results would be helpful to assess the prognosis of patients with PDAC and might offer the promise of individualized therapeutic interventions.

Materials And Methods

Datasets, m6A-Related Genes and Annotation of lncRNAs

For TCGA training dataset, normalized RNA sequencing data [Fragments Per Kilobase of transcript per Million mapped reads (FPKM) normalized] and the corresponding clinicopathological data of PDAC were obtained from the Genomic Data Commons Data Portal (https://portal.gdc.cancer.gov/). To obtain a ICGC validation dataset, normalized RNA-seq data of PACA-AU and the corresponding clinicopathological data were downloaded from the ICGC Data Portal (https://dcc.icgc.org). Only the patients with histological confirmed in PDAC was included, patients with OS < 30 days or unknown OS status were excluded. Finally, we obtained the TCGA training cohort of 140 patients and the ICGC validation cohort of 63 patients. Moreover, on the basis of published literatures, the expression data of 24 m6A-related genes were generated from the TCGA and ICGC datasets, including writers (*METTL3, METTL14, METTL16, RBM15, RBM15B, WTAP, VIRMA [KIAA1429], CBLL1* and *ZC3H13*), erasers (*ALKBH5* and *FTO*) and readers (*YTHDF1, YTHDF2, YTHDF3, YTHDC1, YTHDC2, HNRNPC, HNRNPA2B1, IGF2BP1, IGF2BP2, IGF2BP3, FMR1, RBMX* and *LRPPRC*). In our study, annotation of lncRNAs based on eight types of transcript (lincRNA, antisense, 3prime overlapping ncRNA, processed transcript, sense overlapping, sense intronic and macro lncRNA). Based on the Ensemble IDs and types of the transcript from the GENCODE website (https://www.gencodegenes.org/human/), 14830 lncRNAs were identified in the TCGA cohort and 12559 lncRNAs were identified in the ICGC cohort.

Obtaining m6A-related lncRNAs

Pearson correlation analyses were applied to explore m6A-related lncRNAs (|Pearson R| > 0.4 and $p < 0.001$) in two cohorts. To ensure a more accurate corresponding relationship between m6A-related genes and lncRNAs, the results of correlation were built in “m6A-related gene/lncRNA/positive or negative correlation” format (eg. YTHDF1/ZFAS1/positive). The formatted results from the two cohorts were intersected to generate the 262 m6A-related lncRNAs from 582 correlations.

Identifying prognostic m6A-related lncRNAs

We selected OS as the endpoint. In TCGA training cohort, univariate Cox regression analysis was first conducted to identify the prognostic m6A-related lncRNAs, Next, least absolute shrinkage and selection operator (LASSO) Cox regression analysis was performed using the R package “glmnet” through 10-fold cross-validation. Finally, multivariate Cox regression analysis was conducted to identify the independent prognostic m6A-related lncRNAs. Based on the multivariate Cox regression result, a m6A-related lncRNA prognostic riskscore (m6A-LPR) model was developed for the PADC patients, each patient’s risk score was calculated by a combination of the expression levels of lncRNAs and multivariate Cox regression coefficients in TCGA training cohort. We used the median risk score as the cut-off value to categorize the patients into high-risk group and low-risk group. The ICGC dataset were used as the validation cohort to verify the m6A-LPR. The time-dependent receiver operating characteristic (ROC) curves of the risk scores were conducted using the R package “timeROC” to evaluate the prognostic accuracy of m6A-LPR.

Functional and pathway enrichment analysis

In the TCGA cohort, based on the m6A-LPR, differentially expressed genes (DEGs) between the high-risk group and low-risk group were identified using the R package “limma” (|log2(Fold change)| > 1 and False

Discovery Rate (FDR) < 0.05). The 927 DEGs were obtained and imported into the “Metascape” website (https://metascape.org)[17] for functional and pathway enrichment analysis, including Reactome Gene Sets, Canonical Pathways, Gene Ontology (GO) Biological Processes and Kyoto Encyclopedia of Genes and Genomes Pathway (KEGG pathway).

Tumor Immunity Analyses

Stromal, immune, and estimate scores were calculated using the ESTIMATE algorithm[18] which was generated from the expression data in the TCGA dataset (https://bioinformatics.mdanderson.org/public-software/estimate/), then we evaluated the differences in stromal, immune, and estimate scores between low- and high-risk group of PDAC patients. Furthermore, to infer the relative abundance of tumor-infiltrating immune cells, CIBERSORT deconvolution algorithm[19] was used, with the LM22 set representing 22 kinds of immune cell. We evaluated the differences in the immune infiltration of 22 immune cell subtypes between low- and high-risk group of PDAC patients.

Potential drugs for prognostic m6A-related lncRNAs

We used the Drug-LncRNA Module of the LncMAP database (http://bio-bigdata.hrbmu.edu.cn/LncMAP/)[20] to analyze the relationship between prognostic m6A-related lncRNAs and drugs, FDR less than 0.05 was considered significant. The m6A-related lncRNAs-drugs network was plotted by Cytoscape (version 3.8.2, http://www.cytoscape.org/)[21].

Statistical analysis

All statistical analyses and plots were performed using R Foundation Statistical software (version 4.0.2). Categorical variables were analyzed using χ2 test or Fisher's exact test. Continuous variables were analyzed using Student's t test or Wilcoxon test. Survival was estimated using the Kaplan-Meier survival curves and compared using the log-rank test. Univariate, LASSO and multivariate Cox regression analyses were performed to identify independent prognostic m6A-related lncRNAs and to develop the m6A-LPR. The hazard ratio (HR) and 95% confidence interval (CI) were calculated. Unless otherwise stipulated, two tailed $p < 0.05$ was considered statistically significant.

Results

Identification of m6A-Related lncRNAs in PDAC Patients

The work flow was shown in Fig. 1. Cumulatively, 140 PDAC patients from TCGA cohort and 63 PDAC patients from ICGC cohort were included in our study; for whom, the baseline clinical features were presented in Additional file 1: Table S1. Firstly, we identified 14830 lncRNAs in the TCGA cohort and 12559 lncRNAs in the ICGC cohort. Next, we extracted the expression data of lncRNAs and 24 m6A-related genes from the TCGA and the ICGC cohorts. Pearson correlation analyses were performed to identify m6A-related lncRNAs in two cohorts (|Pearson R| > 0.4 and p < 0.001). We obtained the 2672 correlations in the TCGA cohort and 21008 correlations in ICGC cohorts, then the corresponding

relationship between m6A-related genes and lncRNAs in two cohorts were intersected. Finally, 585 shared correlations were obtained in both two cohorts, then 262 m6A-related lncRNAs were extracted from the shared correlations.

Identification of prognostic m6A-Related lncRNAs

Univariate Cox regression was applied to identify prognostic m6A-related lncRNAs from the 262 m6A-related lncRNAs in the TCGA traing cohort ($p < 0.05$). The result showed that 28 m6A-related lncRNAs were significantly associated with the OS (Fig. 2a), including 2 risky lncRNAs and 26 protective lncRNAs, and the correlations between the 28 lncRNAs and the m6A-related genes in the TCGA cohort are shown in Fig. 2b.

Establishment of the m6A-LPR in the TCGA Training Cohort

To construct the m6A-LPR for predicting the OS of PDAC patients, LASSO Cox analysis was performed to the 28 prognostic m6A-related lncRNAs in the TCGA cohort and 12 m6A-related lncRNAs were screened (Fig. 3a). Next, multivariate Cox proportional regression analysis was performed for analyzing these 12 m6A-related lncRNAs in TCGA cohort to construct the m6A-LPR. The m6A-LPR comprising four m6A-related lncRNAs, including MIR4435-1HG, RP5-1112D6.4, RP11-582J16.5 and RP11-999E24.3, was developed through the summary of the expression values of these four m6A-related lncRNAs multiplied by corresponding coefficients derived from the above multivariable Cox regression analysis (Fig. 3b, c). The downregulated RP5-1112D6.4, RP11-582J16.5, and RP11-999E24.3 with HR < 1 were considered to be tumor suppressors, while the upregulated MIR4435-1HG with HR > 1 was considered to be oncogenes. The Kaplan–Meier survival curves showed that higher expression of RP5-1112D6.4, RP11-582J16.5 and RP11-999E24.3 and lower expression of MIR4435-1HG were correlated with impoved OS in the TCGA cohort (Fig. 3d-g). The expression of four m6A-related lncRNAs were also associated with the clinicopathological and immune signatures of PDAC, such as WHO grade, TP53 mutation status, KRAS mutation status, ESTIMATE score, immune score, stromal score, and tumor mutation burden (TMB) (Fig. 3h). The genomic information of these four m6A-related lncRNAs and the corresponding correlation with m6A regulators were presented in Table 1. The risk score for each patient was calculated by following formula based on m6A-LPR: [(0.205)*expression value of MIR4435-1HG] - [(0.525)*expression value of RP11-582J16.5] - [(0.658)*expression value of RP11-999E24.3] - [(0.275)*expression value of RP5-1112D6.4]. Based on the median value of risk scores, patients were categorized into low-risk and high-risk groups. Kaplan–Meier survival curves showed that PDAC patients with lower risk scores had better OS ($p = 0.0011$) (Fig. 4a). Survival status and risk score distributions were illustrated in Fig. 4b. The ROC curves demonstrated that m6A-LPR had a good performance for predicting OS in the TCGA cohort (1-year AUC = 0.760, 2-year AUC = 0.722; Fig. 4c).

Validation of the m6A-LPR in the ICGC Cohort

In order to further validate the robustness of m6A-LPR, the risk scores were calculated in the ICGC cohort using the above equation. Based on the median risk score, PDAC patients in the ICGC cohort were also divided into low- and high-risk subgroups. Consistent with the results in the TCGA training cohort: PDAC patients with lower risk scores had better OS in the ICGC validation cohort ($p = 0.020$) (Fig. 4d). Survival status and risk score distributions were shown in Fig. 4e. The ROC curves also demonstrated that m6A-LPR had a prognostic value for PDAC patients in the ICGC cohort (1-year AUC = 0.657, 2-year AUC = 0.729; Fig. 4f). These results showed that the m6A-LPR based prognostic signature had a robust and stable ability in prognosis prediction for PDAC.

Principal Component Analysis

Principal component analysis (PCA) was applied to evaluate the discrepancies between the low- and high-risk subgroups based on the expression of the four m6A-related lncRNAs in m6A-LPR (Fig. 5a, b). The results showed that the samples screened by the four m6A-related lncRNAs could clearly divide the whole patients into a low-risk and high-risk group in both the TCGA and ICGC cohorts.

Stratification Analysis of the m6A-LPR in clinicopathological features

PDAC patients with WHO grade III-IV, mutant TP53 and mutant KRAS (Fig. 6a–c) had higher risk scores, whereas the risk scores were not correlated with stage, T category and N category (Fig. 6d-f). To evaluate whether m6A-LPR was an independent prognostic factor for PDAC patients, univariate and multivariate Cox analyses were performed. In the TCGA cohort, univariate Cox analysis showed that m6A-LPR was significantly associated with OS (HR: 2.72, 95% CI: 1.94–3.81, $p < 0.001$) and multivariate Cox analysis indicated that m6A-LPR was an independent predictor of OS (HR: 2.77, 95% CI: 1.93–3.96, $p < 0.001$; Fig. 6g, h). In the ICGC validation cohort, univariate and multivariate Cox analyses also indicated that m6A-LPR was an independent predictor of OS for PDAC patients (univariate: HR: 1.83, 95% CI: 1.12–2.66, $p = 0.012$; multivariate: HR: 1.75, 95% CI: 1.12–2.50, $p = 0.020$; Fig. 6i, j). These results demonstrated that m6A-LPR might be helpful for clinical prognosis evaluation as an independent prognostic indicator.

Stratification Analysis of the m6A-LPR in immune features

The relationship between m6A-LPR and tumor immunity was further evaluated. Tumor purity, TMB, Immune Checkpoint Molecules and the infiltration level of immune cell were estimated. PDAC patients in the high-risk group had remarkably lower stromal, immune, and ESTIMATE scores, indicating a lower level of stroma, immune cell infiltration, and tumor purity (Fig. 7a). Furthermore, PDAC patients in the high-risk group had significantly higher levels of TMB (Fig. 7b) and lower levels of CTLA4 expression (Fig. 7c). To further investigate the underlying molecular mechanisms of the m6A-LPR and its relevance to tumor immunity, the relative abundance of 22 tumor-infiltrating immune cells was assessed for each patient using CIBERSORT. The high-risk group was associated with significantly higher levels of plasma B cells

and resting NK cells infiltration, and lower levels of infiltrating resting memory CD4 T cells, monocytes and resting mast cells (Fig. 7d).

Functional and pathway enrichment analysis

To explore the potential biological processes and pathways of the molecular discrepancy between the low-risk and high-risk groups, 927 differential expression genes (DEGs) were identified between the low-risk and high-risk groups in the TCGA cohort (|log2 (fold change) | > 1 and $p < 0.05$). Functional and pathway enrichment analysis indicated these DEGs were mainly enriched in these aspects: digestion, neuronal system and peptide hormone metabolism (Reactome Gene Sets); NABA matrisome-associated (Canonical Pathways); pancreatic secretion, neuroactive ligand-receptor interaction and cytokine-cytokine receptor interaction (KEGG Pathways); regulation of ion transport, chemical synaptic transmission, regulation of system process, signal release, neuropeptide signaling pathway and second-messenger-mediate signaling (GO Biological Processes) (Fig. 8a–c). These results could give us some insights into the potential molecular mechanisms of the m6A-LPR.

Explore Potential Drugs that have a Therapeutic Effect on PDAC

From the Drug-LncRNA Module of the LncMAP database, we obtained 304304 drug-lncRNA interaction pairs. A total of 28 prognostic m6A-related lncRNAs were then imported into the database to predict the potential drugs of the genes, and 75 drug-lncRNA interactions were extracted when FDR < 0.05. The network including 18 prognostic m6A-related lncRNAs and 18 drugs was identified (Fig. 9). The five most interaction with prognostic m6A-related lncRNAs drugs were Panobinostat, L-685458, Palbociclib, Crizotinib and TAE684.

Discussion

PDAC is an extremely challenging disease, since only 80% of patients with PDAC are not amenable to surgery at diagnosis[3]. Recently, with the benefit of high-throughput sequencing, studies to explore the molecular markers of PDAC at the molecular and cellular level have got breakthroughs, which will be helpful for increasing the prognostic accuracy and introducing potential therapeutic targets for PDAC. An increasing number of studies indicated that epigenetic alterations can largely effect cancer progression[22]. Among that, m6A modification is the most common epigenetic methylated modification of mRNAs and ncRNAs[4], it has been confirmed to play critical regulatory roles in the modification of tumor RNAs[5]. Aberrant lncRNAs had been found to be a important role in the carcinogenicity of PDAC[8,14–16]. However, few studies have been conducted to investigate the mechanisms underlying how lncRNAs are regulated by m6A modification to involve in the onset and development of PDAC Therefore, we tried to identify m6A-related lncRNAs through bioinformatics analysis from two public datasets. Twenty-eight m6A-related lncRNAs had prognostic value, and four of them were screened to bulid an m6A-LPR for

predicting the OS of PDAC patients. Furthermore, we explored the correlation of m6A-LPR with clinicopathological and immune features of PDAC and tried to find potential target drugs for prognostic m6A-related lncRNAs.

Previous studies had shown that the stability of lncRNAs is enhanced by the accumulation of m6A modifications[23], with the binding of low-complexity proteins[24], interactions with m6A readers[8], and additional regulatory mechanisms. Recent studies had demonstrated that m6A modification can regulate oncogenesis and tumor progression in PDAC[7–12], but it is still unclear how m6A modification affects the occurrence and progression of PDAC in a lncRNA-dependent pattern. The m6A eraser ALKBH5 could demethylate the lncRNA KCNK15-AS1 and inhibit KCNK15-AS1-mediated pancreatic cancer cell motility[25]. The m6A reader IGF2BP2 could interact with the lncRNA DANCR and promote cancer stemness-like properties and pancreatic cancer pathogenesis[8]. Studies had shown that m6A modification of lncRNAs may have an effect on the occurrence and progression of cancer and lncRNAs may act as target for m6A regulators to influence aggressive tumor progression. Based on these evidences, we should pay more attention to the interactions between lncRNAs and m6A modifications in order to identify potential therapeutic targets or prognosis markers of cancers.

We identified 28 prognostic m6A-related lncRNAs from TCGA dataset, and four of them were included in the m6A-LPR and validated in ICGC dataset. RP5-1112D6.4, RP11-582J16.5, and RP11-999E24.3 were protective genes, MIR4435-1HG was risky gene. MIR4435-1HG is highly expressed and acts as a risky gene in renal cell carcinoma, and it promotes cell proliferation, migration and invasive capacity of renal carcinoma cells[26]. The other three lncRNAs have not been reported in the literatures and the functions of them are unknown. We performed functional analysis of the DEGs in low- and high-risk patients stratified by m6A-LPR to explore the role of four m6A-related lncRNAs in PDAC. The analysis revealed that four m6A-related lncRNAs were significantly enriched in cell ion exchange (regulation of ion transport, inorganic ion homeostasis and anion transport) and biological processes of signaling pathways (neuroactive ligand-receptor interaction, signal release, cytokine-cytokine receptor interaction, neuropeptide signaling pathway and second-messenger-mediated signaling). The result implied that the m6A-LPR might be related to maintain cellular homeostasis and cell injury, thus affecting the progression of the tumor. The findings are probably used to develop new targeted anti-cancer therapies for PDAC if the hypothesis can be proved.

In many types of tumors, such as skin melanoma, breast cancer, colon cancer and non-small cell lung cancer, tumor immune infiltrating cells account for a high proportion based on lncRNA sequencing data[27]. The lncRNA lnc-EGFR can stimulate T-regulatory cells differentiation thus promoting hepatocellular carcinoma immune evasion[28]. LINC00473 can drive the progression of pancreatic cancer via upregulating PD-L1[29]. We believe that lncRNAs are the key to tumor immunotherapy. Therefore, we explored the relationship between m6A-LPR and tumor immunity, and we found that m6A-LPR for PDAC was associated with TMB, tumor purity, and the infiltration of immune cell subtypes.

This study included two PDAC datasets, the TCGA and ICGC datasets, and m6A-LPR containing four prognostic m6A-related lncRNAs were built in the TCGA dataset and validated in the ICGC dataset, but there were several limitations in our study. First, the interactions between lncRNAs and m6A-related genes were obtained from two datasets in our study, them should be confirmed through *in vivo* and *in vitro* experiments. Second, in two datasets, the clinical data are incomplete and exist selection bias. Third, traditional statistical analyzes were used to construct and validate the prognostic risk model of m6A-LPR. Although these methods had been utilized and validated in many studies, it is crucial to improve further studies with more advanced methodologies. To further verify our bioinformatics results, in-depth studies on the m6A-LPR containing four prognostic m6A-related lncRNAs, including molecular mechanisms and functional experiments, are needed.

Conclusion

In summary, we built and validated a prognostic model of m6A-LPR containing four prognostic m6A-related lncRNAs. The m6A-LPR not only provides additional information for PDAC prognostic analyses, but also affects the immunity of PDAC. Further studies are needed to validate our model and to explore the molecular mechanism and function of m6A-LPR in the regulation of anti-tumor immunity, our results may provide some clues for further studies.

Abbreviations

PDAC: Pancreatic ductal adenocarcinoma; m6A: N6-methylandenosine; TCGA: The Cancer Genome Atlas; ICGC: International Cancer Genome Consortium; LASSO: least absolute shrinkage and selection operator; m6A-LPR: m6A-related lncRNAs prognostic riskscore; OS: overall survival; ROC: receiver operating characteristic; mRNAs: messenger RNAs; lncRNAs: Long non-coding RNAs; FPKM: Fragments Per Kilobase of transcript per Million; DEGs: differentially expressed genes; FDR: False Discovery Rate; GO: Gene Ontology; KEGG: Kyoto Encyclopedia of Genes and Genomes; HR: hazard ratio; CI: confidence interval; TMB: tumor mutation burden.

Declarations

Acknowledgements

Not applicable.

Authors' contributions

YuHai Hu performed the collection, assembly and interpretation of data, edited the manuscript; YiPing Chen wrote the manuscript, designed the study and confirmed the data presented in the manuscript. All authors read and approved the final manuscript.

Funding

Not applicable.

Availability of data and materials

TCGA training data was downloaded from the TCGA database (http://cancergenome.nih.gov) under the accession number TCGA-PAAD. ICGC validation data was downloaded from the ICGC database (https://dcc.icgc.org) under the accession number PACA-AU.

Ethics approval and consent to participate

Not applicable.

Consent for publication

Not applicable.

Competing interests

The authors declare that they have no competing interests.

References

1 Quaresma, M., Coleman, M. P. & Rachet, B. 40-year trends in an index of survival for all cancers combined and survival adjusted for age and sex for each cancer in England and Wales, 1971-2011: a population-based study. *Lancet***385**, 1206-1218, doi:10.1016/s0140-6736(14)61396-9 (2015).

2 Bates, S. E. Pancreatic Cancer: Challenge and Inspiration. *Clinical cancer research : an official journal of the American Association for Cancer Research***23**, 1628, doi:10.1158/1078-0432.ccr-16-2069 (2017).

3 Strobel, O., Neoptolemos, J., Jäger, D. & Büchler, M. W. Optimizing the outcomes of pancreatic cancer surgery. *Nature reviews. Clinical oncology***16**, 11-26, doi:10.1038/s41571-018-0112-1 (2019).

4 Fu, Y., Dominissini, D., Rechavi, G. & He, C. Gene expression regulation mediated through reversible m□A RNA methylation. *Nature reviews. Genetics***15**, 293-306, doi:10.1038/nrg3724 (2014).

5 Pan, Y., Ma, P., Liu, Y., Li, W. & Shu, Y. Multiple functions of m(6)A RNA methylation in cancer. *Journal of hematology & oncology***11**, 48, doi:10.1186/s13045-018-0590-8 (2018).

6 Zaccara, S., Ries, R. J. & Jaffrey, S. R. Reading, writing and erasing mRNA methylation. *Nature reviews. Molecular cell biology***20**, 608-624, doi:10.1038/s41580-019-0168-5 (2019).

7 Guo, X. *et al.* RNA demethylase ALKBH5 prevents pancreatic cancer progression by posttranscriptional activation of PER1 in an m6A-YTHDF2-dependent manner. *Molecular cancer***19**, 91, doi:10.1186/s12943-020-01158-w (2020).

8 Hu, X. *et al.* IGF2BP2 regulates DANCR by serving as an N6-methyladenosine reader. *Cell death and differentiation***27**, 1782-1794, doi:10.1038/s41418-019-0461-z (2020).

9 Tang, B. *et al.* m(6)A demethylase ALKBH5 inhibits pancreatic cancer tumorigenesis by decreasing WIF-1 RNA methylation and mediating Wnt signaling. *Molecular cancer***19**, 3, doi:10.1186/s12943-019-1128-6 (2020).

10 Tian, J. *et al.* N(6)-methyladenosine mRNA methylation of PIK3CB regulates AKT signalling to promote PTEN-deficient pancreatic cancer progression. *Gut***69**, 2180-2192, doi:10.1136/gutjnl-2019-320179 (2020).

11 Wang, M. *et al.* Upregulation of METTL14 mediates the elevation of PERP mRNA N(6) adenosine methylation promoting the growth and metastasis of pancreatic cancer. *Molecular cancer***19**, 130, doi:10.1186/s12943-020-01249-8 (2020).

12 Zhang, J. *et al.* Excessive miR-25-3p maturation via N(6)-methyladenosine stimulated by cigarette smoke promotes pancreatic cancer progression. *Nature communications***10**, 1858, doi:10.1038/s41467-019-09712-x (2019).

13 Schmitt, A. M. & Chang, H. Y. Long Noncoding RNAs in Cancer Pathways. *Cancer cell***29**, 452-463, doi:10.1016/j.ccell.2016.03.010 (2016).

14 Li, Z. H. *et al.* The long non-coding RNA HOTTIP promotes progression and gemcitabine resistance by regulating HOXA13 in pancreatic cancer. *Journal Of Translational Medicine***13**, doi:10.1186/s12967-015-0442-z (2015).

15 Ma, C. C. *et al.* H19 promotes pancreatic cancer metastasis by derepressing let-7's suppression on its target HMGA2-mediated EMT. *Tumor Biology***35**, 9163-9169, doi:10.1007/s13277-014-2185-5 (2014).

16 Pang, E. J., Yang, R., Fu, X. B. & Liu, Y. F. Overexpression of long non-coding RNA MALAT1 is correlated with clinical progression and unfavorable prognosis in pancreatic cancer. *Tumor Biology***36**, 2403-2407, doi:10.1007/s13277-014-2850-8 (2015).

17 Zhou, Y. *et al.* Metascape provides a biologist-oriented resource for the analysis of systems-level datasets. *Nature communications***10**, 1523, doi:10.1038/s41467-019-09234-6 (2019).

18 Yoshihara, K. *et al.* Inferring tumour purity and stromal and immune cell admixture from expression data. *Nature communications***4**, 2612, doi:10.1038/ncomms3612 (2013).

19 Gentles, A. J. *et al.* The prognostic landscape of genes and infiltrating immune cells across human cancers. *Nature medicine***21**, 938-945, doi:10.1038/nm.3909 (2015).

20 Li, Y. *et al.* LncMAP: Pan-cancer atlas of long noncoding RNA-mediated transcriptional network perturbations. *Nucleic acids research***46**, 1113-1123, doi:10.1093/nar/gkx1311 (2018).

21 Shannon, P. *et al.* Cytoscape: a software environment for integrated models of biomolecular interaction networks. *Genome research***13**, 2498-2504, doi:10.1101/gr.1239303 (2003).

22 Ilango, S., Paital, B., Jayachandran, P., Padma, P. R. & Nirmaladevi, R. Epigenetic alterations in cancer. *Frontiers in bioscience (Landmark edition)***25**, 1058-1109 (2020).

23 Ni, W. *et al.* Long noncoding RNA GAS5 inhibits progression of colorectal cancer by interacting with and triggering YAP phosphorylation and degradation and is negatively regulated by the m(6)A reader YTHDF3. *Molecular cancer***18**, 143, doi:10.1186/s12943-019-1079-y (2019).

24 Hazra, D., Chapat, C. & Graille, M. m⁶A mRNA Destiny: Chained to the rhYTHm by the YTH-Containing Proteins. *Genes***10**, doi:10.3390/genes10010049 (2019).

25 He, Y. *et al.* ALKBH5 Inhibits Pancreatic Cancer Motility by Decreasing Long Non-Coding RNA KCNK15-AS1 Methylation. *Cellular physiology and biochemistry : international journal of experimental cellular physiology, biochemistry, and pharmacology***48**, 838-846, doi:10.1159/000491915 (2018).

26 Wu, K. *et al.* Long non-coding RNA MIR4435-1HG promotes cancer growth in clear cell renal cell carcinoma. *Cancer biomarkers : section A of Disease markers***29**, 39-50, doi:10.3233/cbm-201451 (2020).

27 Yu, W. D., Wang, H., He, Q. F., Xu, Y. & Wang, X. C. Long noncoding RNAs in cancer-immunity cycle. *Journal of cellular physiology***233**, 6518-6523, doi:10.1002/jcp.26568 (2018).

28 Jiang, R. *et al.* The long noncoding RNA lnc-EGFR stimulates T-regulatory cells differentiation thus promoting hepatocellular carcinoma immune evasion. *Nature communications***8**, 15129, doi:10.1038/ncomms15129 (2017).

29 Zhou, W. Y. *et al.* Long noncoding RNA LINC00473 drives the progression of pancreatic cancer via upregulating programmed death-ligand 1 by sponging microRNA-195-5p. *Journal of cellular physiology***234**, 23176-23189, doi:10.1002/jcp.28884 (2019).

Table

Due to technical limitations, Table 1 is only available as a download in the supplementary files section.

Figures

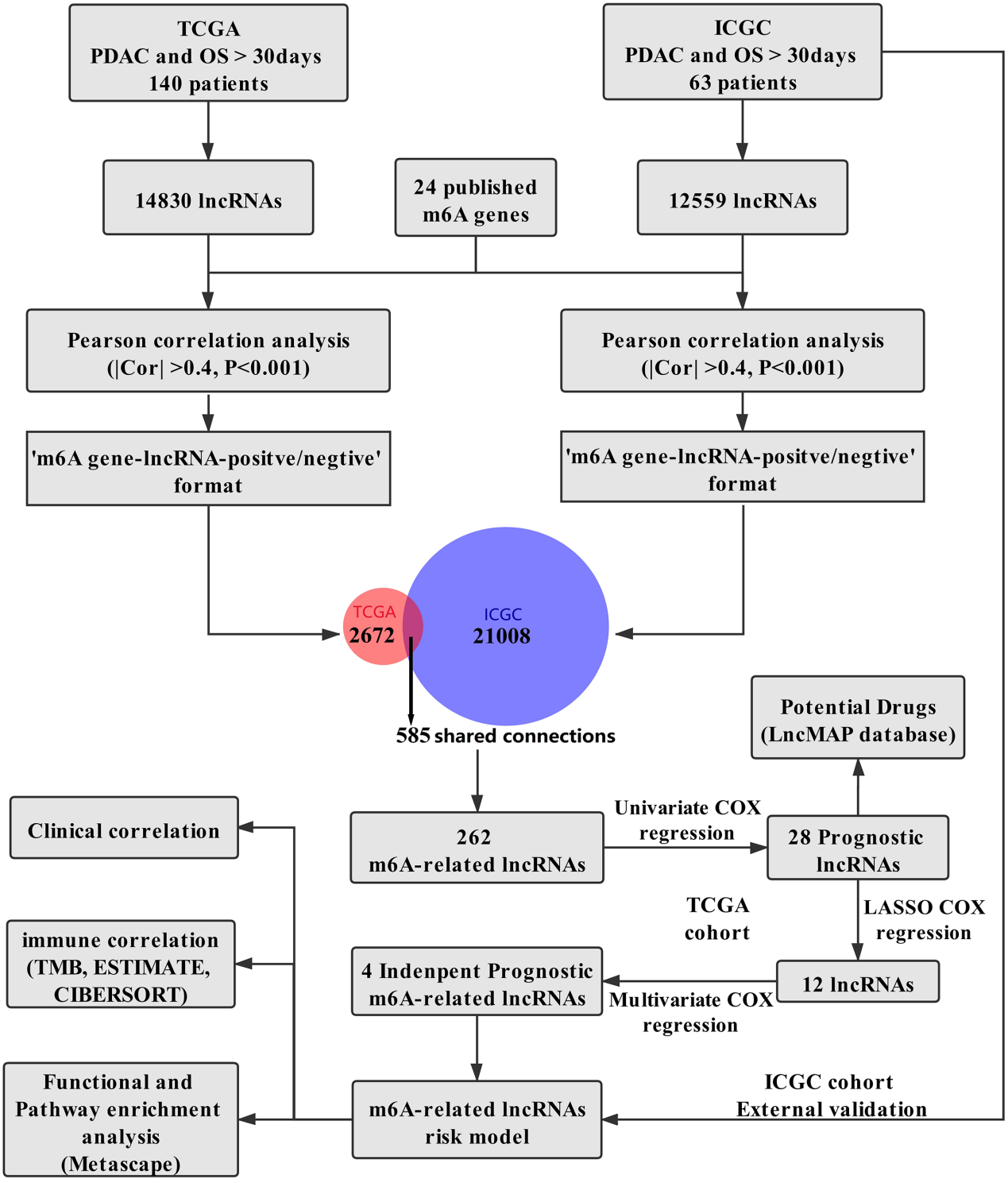

Figure 1

Flow chart of this study.

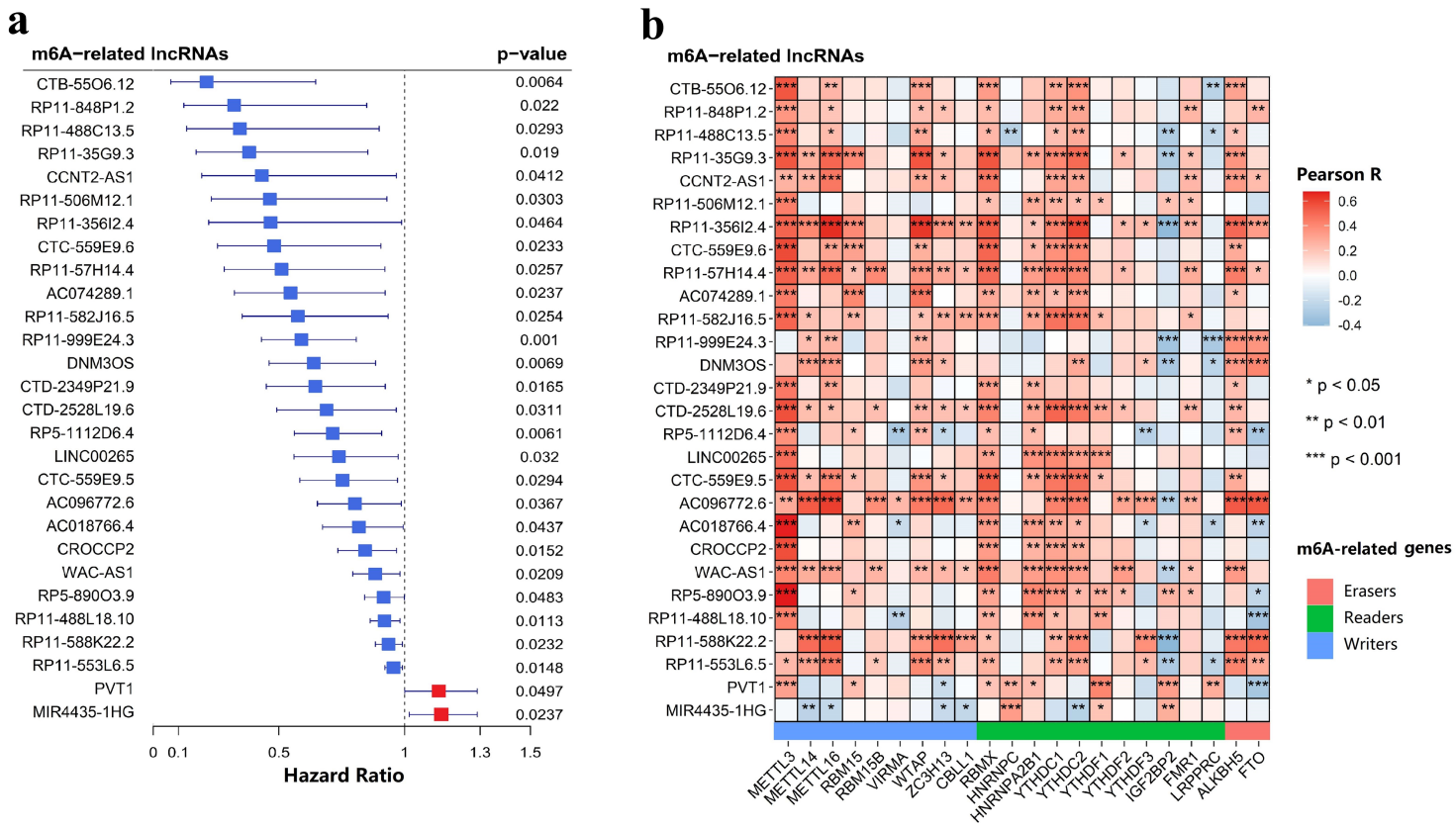

Figure 2

The 28 prognostic m6A-related lncRNAs. a The twenty-eight prognostic m6A-related lncRNAs in The Cancer Genome Atlas (TCGA) cohort. b Heatmap of the correlations between m6A-related genes and the 28 prognostic m6A-related lncRNAs.

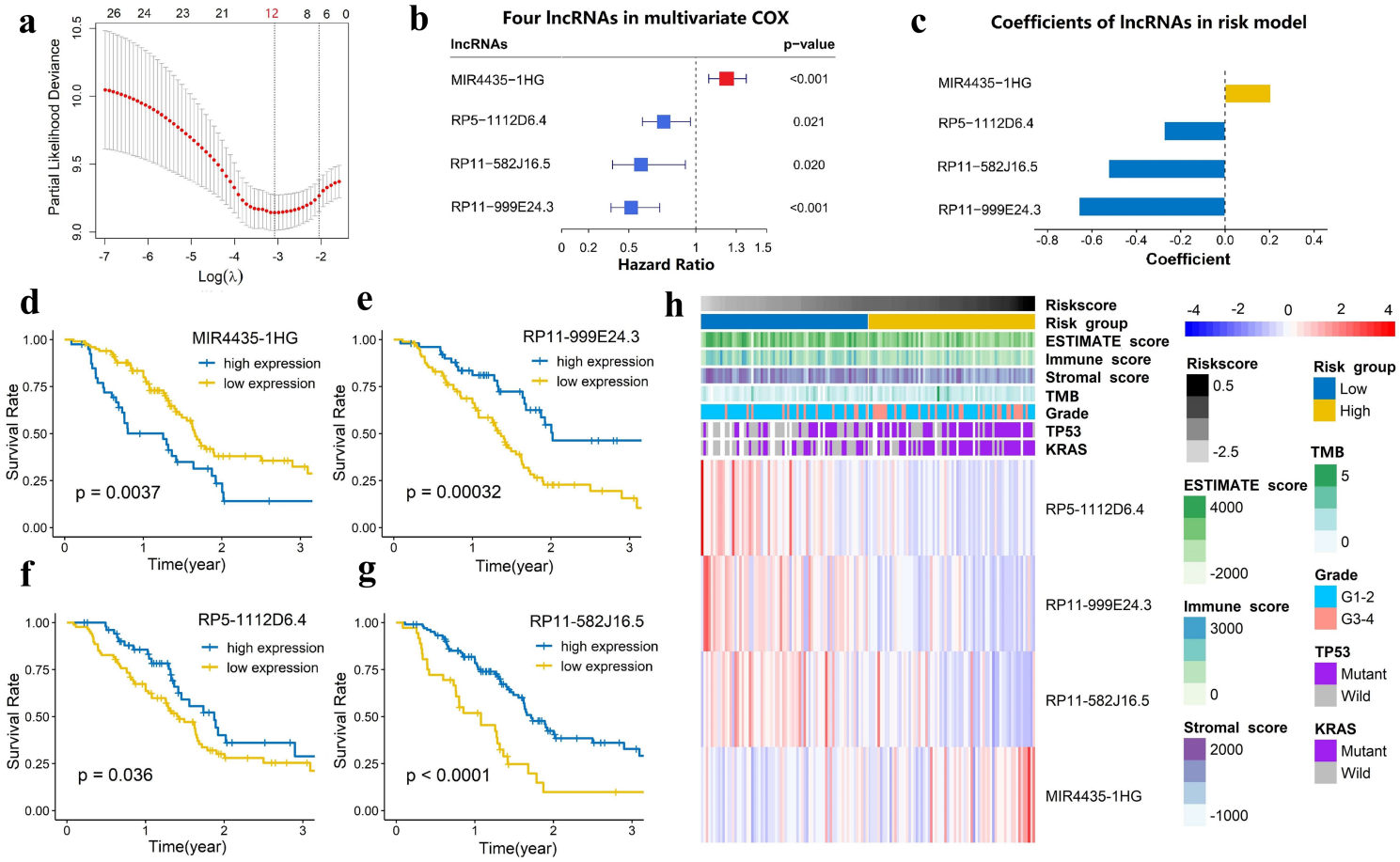

Figure 3

Four m6A-related lncRNAs in risk model were identified by Least absolute shrinkage and selection operator (LASSO) regression and Multivariate cox regression. a LASSO regression was performed, calculating the minimum criteria. b-c Multivariate cox regression was performed, calculating the hazard ratio (HR), p value (b) and and coefficients (c) for four m6A-related lncRNAs in risk model. d–g Kaplan–Meier curves showing that patients with different expression levels of the four m6A-related lncRNAs had different overall survival. h Heatmap of the associations between the expression levels of the four m6A-related lncRNAs and clinicopathological features in The Cancer Genome Atlas (TCGA) cohort.

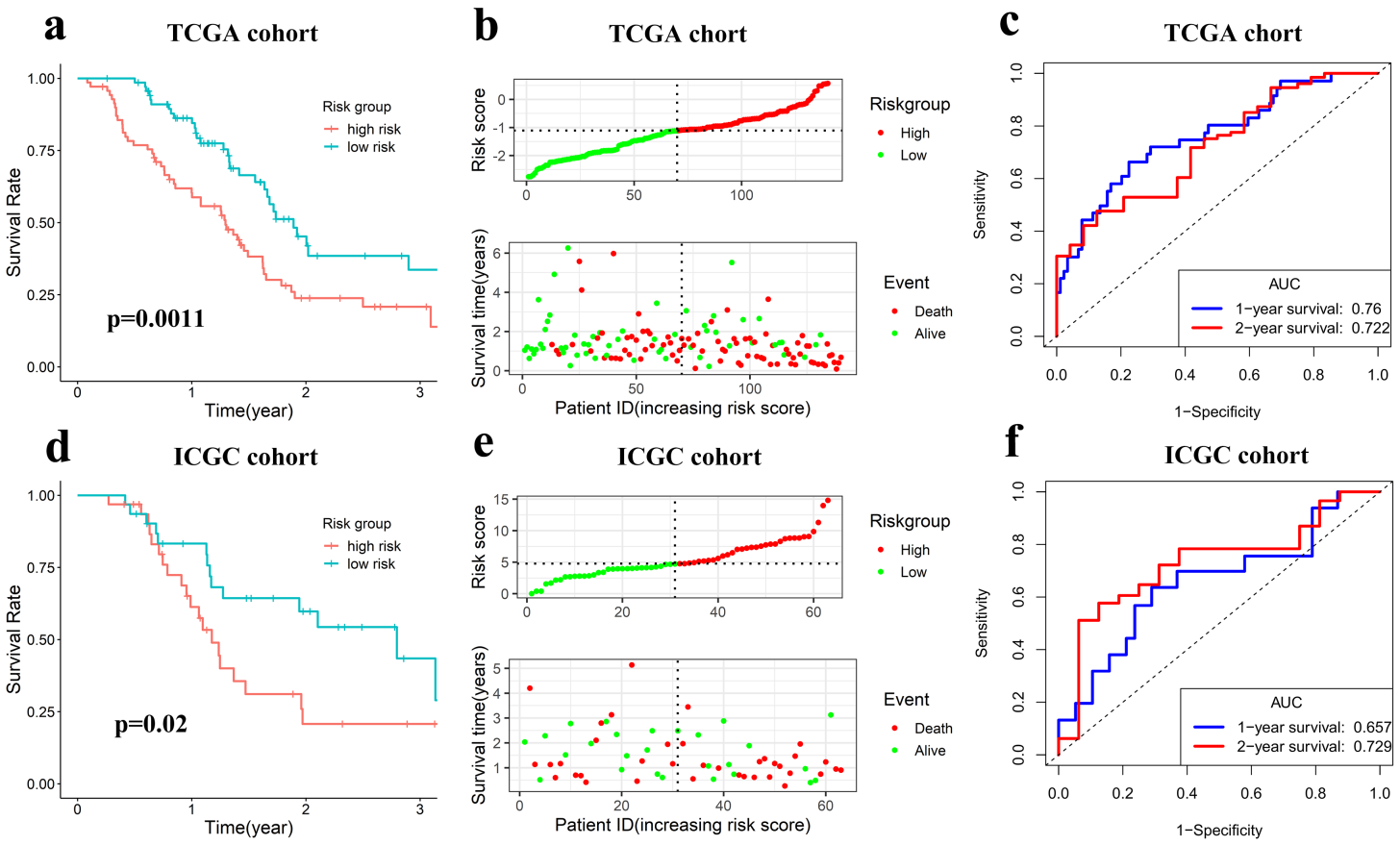

Figure 4

The m6A-related lncRNA prognostic riskscore (m6A-LPR) in training cohort and validation cohort. a Kaplan–Meier curves showed that the high-risk group had worse overall survival than the low-risk group in the training cohort. b Distributions of risk scores based on the m6A-LPR and survival status of patients in the training cohort. c Receiver operating characteristic (ROC) curves of m6A-LPR for predicting the 1/2-year survival in the training cohort. d Kaplan–Meier curves showing that the high-risk group had worse overall survival than the low-risk group in the validation cohort. e Distributions of risk scores and survival status of patients in the validation cohort. f ROC curves of m6A-LPR for predicting 1/2-year survival in the validation cohort.

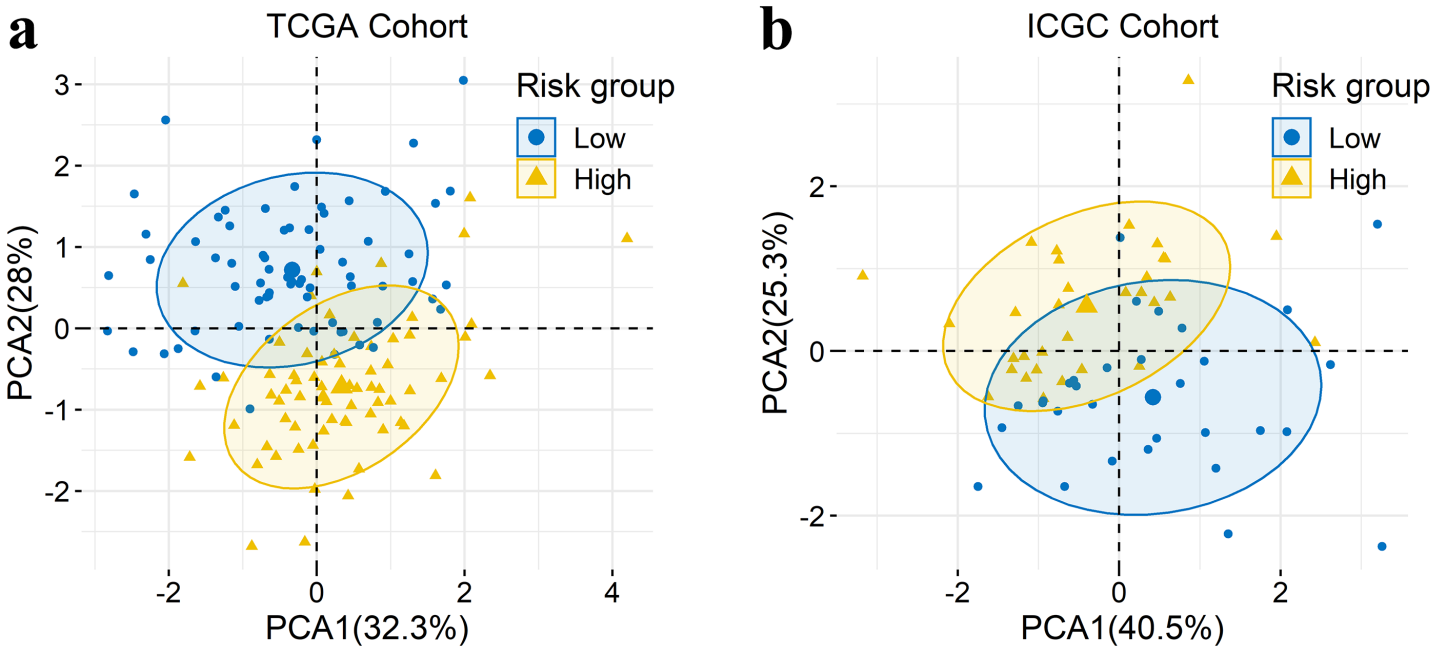

Figure 5

Principal component analysis (PCA) between the low- and high-risk groups based on the expression of the four m6A-related lncRNAs in the m6A-related lncRNA prognostic riskscore (m6A-LPR) in the training cohort (a) and the validation cohort (b).

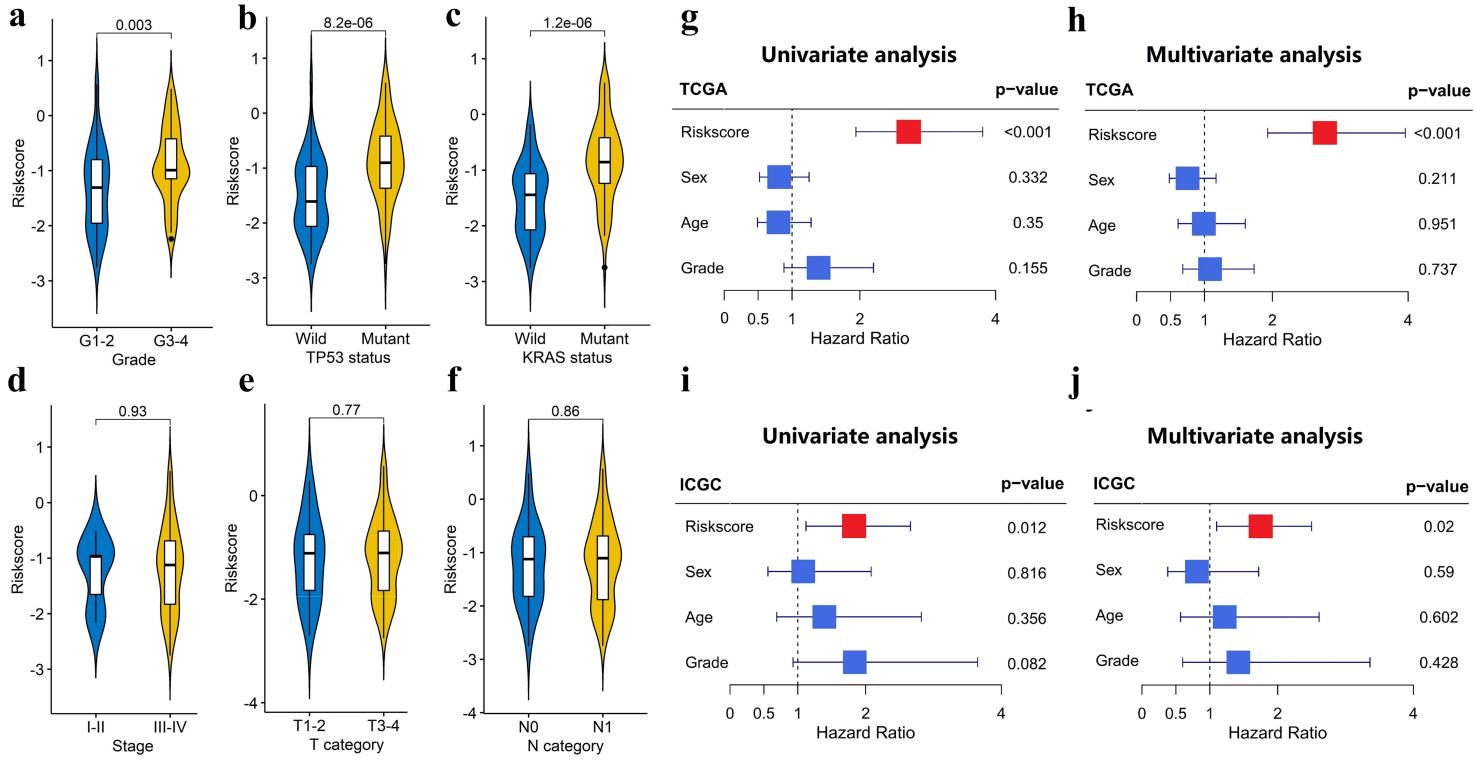

Figure 6

Stratification Analysis of the m6A-related lncRNA prognostic riskscore (m6A-LPR) in clinicopathological features. a–f Patients with different clinicopathological features (including grade, TP53 status and KRAS status, but not stage, T category and N category) had different levels of riskscore, calculated based on the m6A-LPR. g-j Univariate and multivariate analyses revealed that riskscore was an independent prognostic predictor in the training (g, h) and validation (i, j) cohorts.

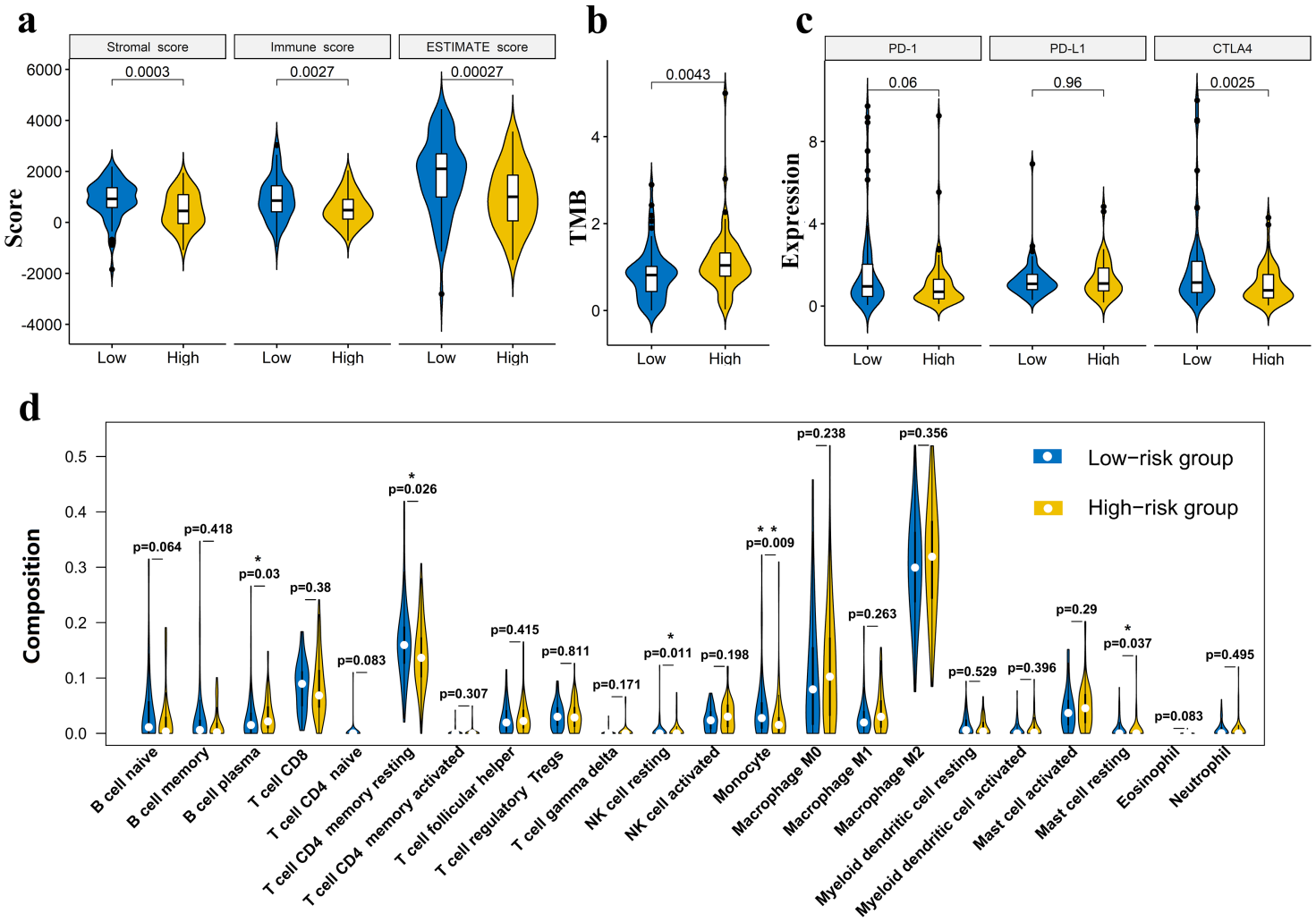

Figure 7

Stratification Analysis of the m6A-related lncRNA prognostic riskscore (m6A-LPR) in immune features. a-b The stromal score, immune score, tumor purity and tumor mutation burden (TMB) significantly differ between the low- and high-risk groups based on the m6A-LPR in the training cohort. c Comparison of the expression pattern of immune checkpoint genes (PD1, PD-L1, and CTLA-4) between the low- and high-risk groups based on the m6A-LPR in the training cohort. d Relative infiltrating proportion of immune cells in low- and high-risk groups.

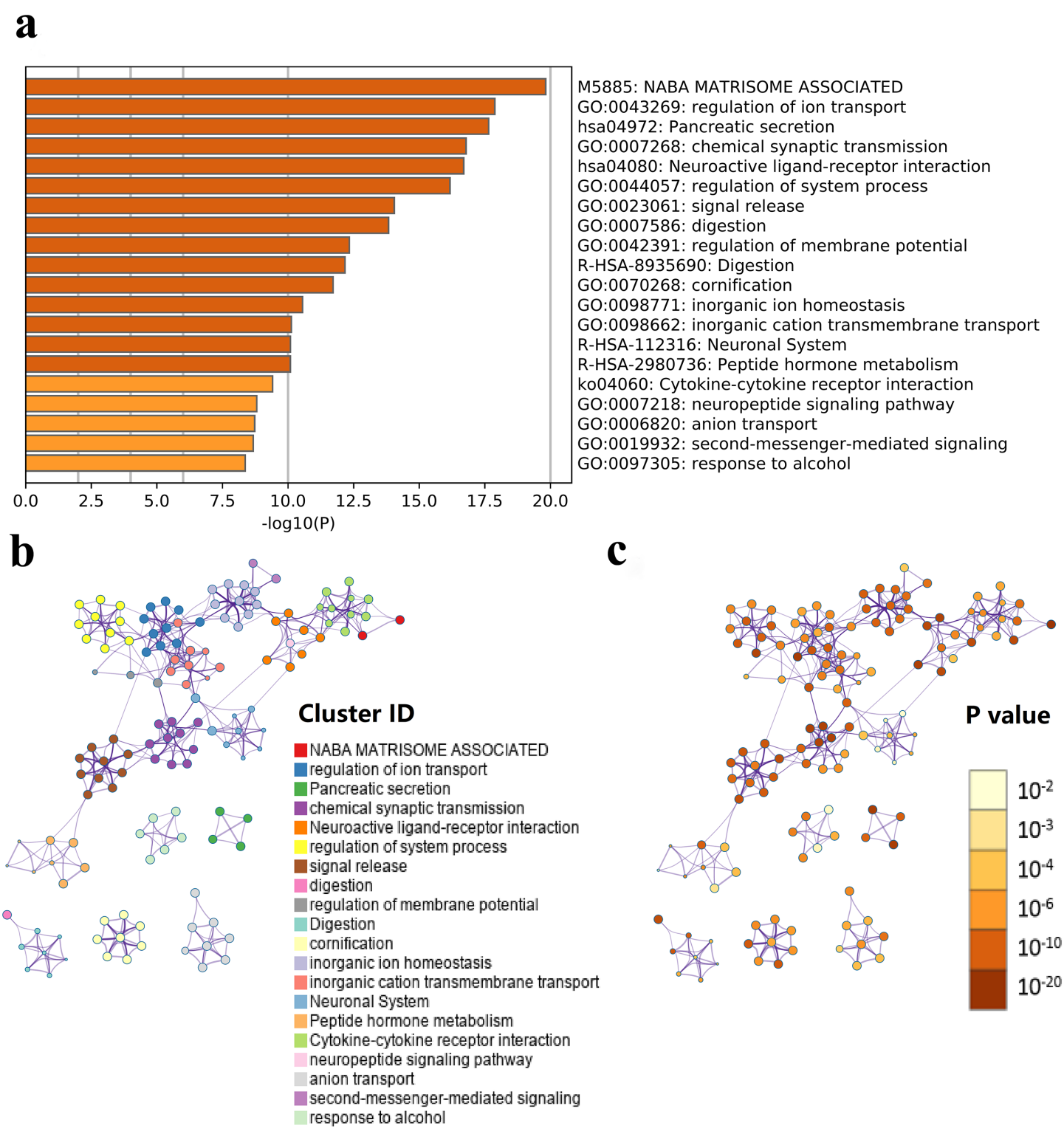

Figure 8

Functional analysis of 927 differentially expressed genes (DEGs) between the low- and high-risk groups. a Heatmap of enriched terms across the inputted gene list, colored according to p-value. Network of enriched terms colored according to cluster ID (b nodes with the same cluster ID are typically close to each other) and p-value (c terms with more genes tend to have higher p-values).

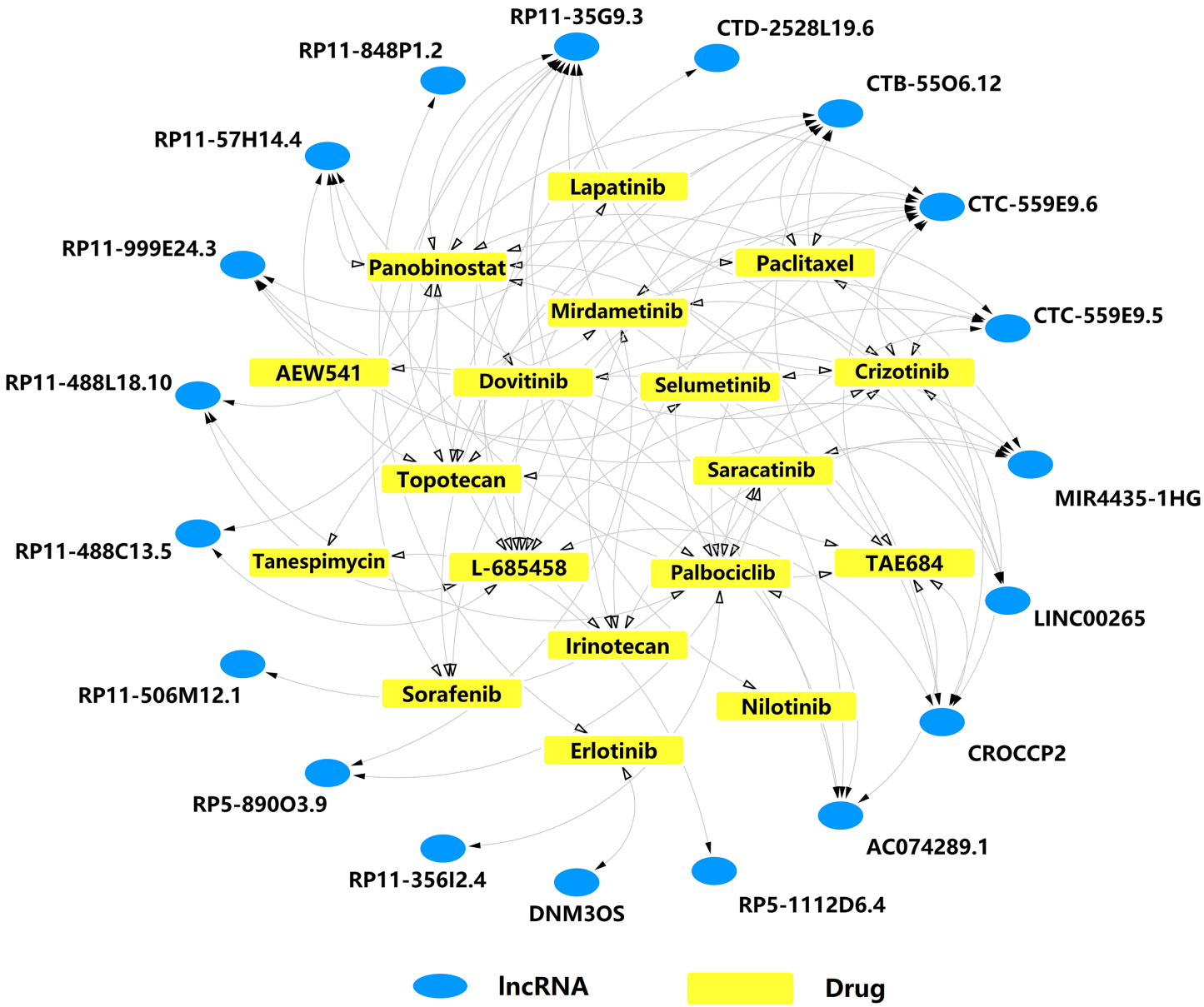

Figure 9

Potential targeted drugs for prognostic m6A-related lncRNAs in the Drug-LncRNA Module of the LncMAP database (False Discovery Rate (FDR) < 0.05

Supplementary Files

This is a list of supplementary files associated with this preprint. Click to download.

- Additionalfile1TableS1.xlsx
- Additionalfile1TableS1.xlsx